Journal of Power Sources 229 (2013) 65–71

Contents lists available at SciVerse ScienceDirect

Journal of Power Sources

journal homepage: www.elsevier.com/locate/jpowsour

Impact of acrylonitrile poisoning on oxygen reduction reaction at Pt/C catalysts

Mohamed S. El-Deab [a,b], Fusao Kitamura [a], Takeo Ohsaka [a,*]

[a] Department of Electronic Chemistry, Interdisciplinary Graduate School of Science and Engineering, Tokyo Institute of Technology, 4259 Nagatsuta, Midori-ku, Yokohama 226-8502, Japan
[b] Department of Chemistry, Faculty of Science, Cairo University, Cairo, Egypt

HIGHLIGHTS

- The influence of acrylonitrile (AcN) on the ORR at a Pt/C catalyst is investigated.
- A few ppm of AcN shifts the onset potential of the ORR and produces more H_2O_2.
- AcN blocks the active sites and affects the work function of the Pt/C.
- The poisoned Pt/C is recovered via a few CV cycles.

ARTICLE INFO

Article history:
Received 28 September 2012
Received in revised form
21 November 2012
Accepted 24 November 2012
Available online 29 November 2012

Keywords:
Nanoparticles
Fuel cells
Oxygen reduction
Poisoning effect
Hydrocarbon impurities

ABSTRACT

This study addresses the poisoning effect of acrylonitrile (AcN) on the catalytic activity of a Pt/C catalyst modified GC disk electrode toward the oxygen reduction reaction (ORR) in O_2-saturated 0.1 M $HClO_4$ solution. A significant retarding effect of AcN on the catalytic performance of the Pt/C catalyst toward the ORR is observed. For instance, the presence of 1 ppm AcN in solution causes a cathodic shift of the half-wave potential of the ORR by ca. 85 mV with the formation of hydrogen peroxide (2-electron reduction product of O_2). Similar Tafel slopes (close to −68 mV dec^{-1}) are obtained at the unpoisoned and the poisoned Pt/C catalysts at low current density region. Whereas, a larger Tafel slope (ca. −228 mV dec^{-1}) is observed at the poisoned catalyst than that obtained at the unpoisoned Pt/C catalyst (ca. −128 mV dec^{-1}) at high current density region. The adsorption of AcN on the surface of the Pt/C is believed to alter its work function (Φ) in such a way that deteriorates its catalytic activity. The recovery of the performance of the Pt/C catalyst is achieved by employing a few potential cycles between the onset potentials of the hydrogen and the oxygen evolution reactions.

1. Introduction

Polymer electrolyte membrane fuel cells (PEMFCs) represent a promising entry into the era of safe, noiseless and eco-friendly energy production devices. PEMFCs are characterized by low operating temperature, fast start-up, high energy conversion efficiency and zero emission. However, their commercialization faces several challenges, e.g., high cost of the Pt catalyst, slow kinetics of the oxygen reduction reaction (ORR), degradation and/or agglomeration of the Pt catalyst which reduces the life-time of PEMFCs. Furthermore, a major source of efficiency loss of PEMFCs is the deterioration of the catalytic activity of the Pt catalyst by inevitable organic and/or inorganic contaminants entering the cell with air, e.g., NOx, SOx and/or hydrocarbons impurities [1–5]. Also, the contamination of the cathode by anode-crossover contaminants is a feasible source of impurities due to the use of a thin Nafion membrane [6,7]. The influence of several individual contaminants on the kinetics of the ORR at Pt nanoparticle-based cathodes has been reported [8–13], for a better understanding of the deterioration and recovery of the fuel cell performance. For instance, the poisoning effect of SO_2 and H_2S on the performance of H_2/Air (O_2) PEMFCs [14–19] and the poisoning effect of nitrogen oxides (NOx) on the ORR at Pt/C catalysts [8,9,20–24] have been investigated. St-Pierre et al. [4] reported a significant loss of PEMFCs performance in the presence of some airborne hydrocarbon contaminants, (e.g., acetonitrile and toluene) which is restored upon exposure to fresh (i.e., contaminant-free) air.

In this context, the current study aims at elucidation of the poisoning effect of acrylonitrile (AcN, in ppm concentration range) on the ORR at a commercially-available Pt/C catalyst in O_2-saturated 0.1 M $HClO_4$ solution. AcN is shown as a possible hydrocarbon

* Corresponding author. Tel.: +81 45 924 5404; fax: +81 45 924 5489.
E-mail addresses: msaada68@yahoo.com (M.S. El-Deab), ohsaka@echem.titech.ac.jp (T. Ohsaka).

0378-7753/$ – see front matter © 2012 Elsevier B.V. All rights reserved.
http://dx.doi.org/10.1016/j.jpowsour.2012.11.100

contaminant from the materials making up the balance of plant (BOP) of PEMFCs such as accessories, piping, blowers, pumps and heat exchanger [5]. Consequently, the impact of AcN on the ORR kinetics is studied herein using steady-state voltammetry. A significant negative shift of the onset potential and the half wave potential ($E_{1/2}$) of the ORR is observed in the presence of a minute amount ($\leq$1 ppm) of AcN in the electrolyte. The activity of the poisoned Pt/C catalyst is restored by cycling the potential between the onset potentials of the hydrogen and oxygen evolution reactions.

2. Experimental

Pt/C catalyst TEC 10E50E (46 wt% Pt) – purchased from Tanaka Kikinzoku Kogyo, Japan – has the following physical characteristics: average particle size of 2.6 nm, Pt surface area of 132.6 $m^2\ g^{-1}$ Pt, and a total BET area of 316.1 $m^2\ g^{-1}$ of catalyst. A thin film electrode of the Pt/C catalyst was used as the working electrode, which was prepared as follows: 8.8 mg Pt/C catalyst was mixed with 1.13 ml H_2O + 0.297 ml isopropanol + 0.092 ml of 5 wt% Nafion and sonicated for 60 min to form the ink, and then 10 μl of the suspension was carefully casted onto the GC disk susbtrate (6 mm in diameter) to fabricate a homogenous film of the Pt/C ink and left for drying for 2 h at room temperature. This gives a film with a loading of 95 μg Pt cm^{-2} of the geometric area of GC electrode. Several investigations are found in literature dealing with the catalytic performance of Pt/C catalysts with loadings ranging from 3.5 to 105 μg Pt cm^{-2} under several operating conditions [25–27]. The loading of 95 μg Pt cm^{-2} is used in the current study as an example to explore the influence of AcN on the ORR at a Pt/C catalyst in 0.1 M $HClO_4$ solution. Prior to casting of the Pt/C ink, the GC disk was polished with no. 2000 emery paper, and then with aqueous slurries of successively finer alumina powder (particle size down to 0.06 μm) with the help of a polishing microcloth, followed with ultrasonic cleaning in milli-Q water for 10 min. The thus-prepared Pt/C catalyst was used as the working electrode for the ORR in O_2-saturated 0.1 M $HClO_4$ solutions containing various amounts of AcN, namely: 0, 0.5, 1, 10 and 100 ppm. A spiral Pt wire and an Ag/AgCl/KCl (sat) were used as the counter and reference electrodes, respectively. A salt bridge is used to eliminate the possibility of contamination with chloride ions from the reference electrode compartment. This salt bridge connects the main compartment of the cell through a Luggin-capillary with the reference electrode. The potentials are reported versus the reversible hydrogen electrode (RHE). *IR*-drop correction of the measured potentials is done by determining the solution resistance (R) by impedance measurements at open circuit potential (ca. 0.98 V vs. RHE). A value of $R = 14.8\ \Omega$ was estimated and assumed constant during the measurements. All the measurements were carried out at room temperature (25 ± 1 °C). A conventional three-electrode cell with a total volume of around 25 ml was used for the cyclic voltammetric (CV) measurements. For hydrodynamic voltammetric measurements, the working electrode compartment was 200 cm^3 to eliminate any possible change in the O_2 concentration during the measurements. Steady-state voltammograms were obtained at a rotating ring-disk electrode (RRDE) with a GC disk (6 mm in diameter) modified with Pt/C catalyst and a Pt ring using a rotary system from Nikko Keisoku, Japan. The Pt/C ink was casted onto the GC disk electrode as described above. Prior to each experiment, O_2 gas was bubbled directly into the cell for 30 min to obtain O_2-saturated solutions, and during the measurements O_2 gas was flushed over the cell solution. Electrolyte solutions were, if necessary, deaerated by bubbling N_2 gas for at least 30 min prior to electrochemical measurements. Electrochemical measurements were performed using a CHI 760/d electrochemical analyzer. The current density was calculated on the basis of the geometric surface area of the underlying GC electrode (= 0.283 cm^2).

3. Results and discussion

3.1. Characterization of Pt/C

Fig. 1A shows typical CVs of a Pt/C catalyst supported on the GC disk electrode in N_2-saturated 0.1 M $HClO_4$ in the presence of various concentrations of AcN measured at a potential scan rate of 0.1 V s^{-1}. Each voltammogram corresponds to the first potential scan at a freshly prepared Pt/C catalyst modified GC electrode in the presence of various concentrations of AcN. Curve a (measured in the absence of AcN) shows a characteristic behavior of a Pt/C catalyst with a broad oxidation peak for the Pt oxide formation

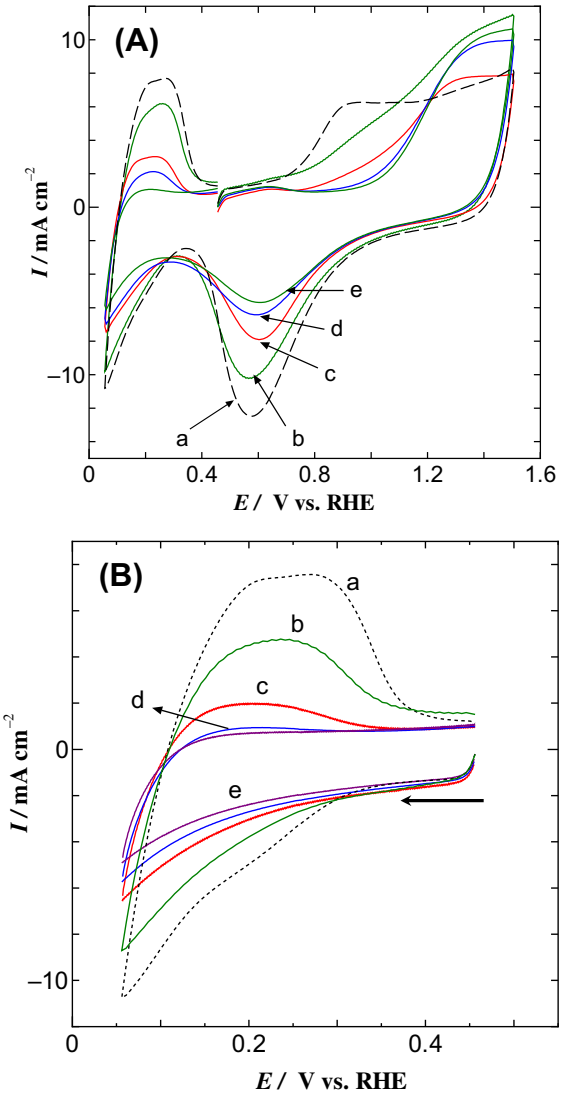

Fig. 1. (A) CVs of the Pt/C catalyst (loaded on GC disk electrode at 95 μg Pt cm^{-2}) in N_2-saturated 0.1 M $HClO_4$ solutions containing (a) 0, (b) 0.5, (c) 1, (d) 10, and (e) 100 ppm acrylonitrile. N.B. each CV corresponds to the 1st potential scan obtained at a freshly prepared Pt/C catalyst-coated GC electrode in the presence of various concentrations of AcN. Potential scan rate: 0.1 V s^{-1} (B) CVs for the hydrogen adsorption-desorption obtained at Pt/C catalyst (loaded on GC disk electrode at 95 μg Pt cm^{-2}) in N_2-saturated 0.1 M $HClO_4$ solutions containing (a) 0, (b) 0.5, (c) 1, (d) 10 and (e) 100 ppm AcN. Each voltammogram corresponds to the first potential scan at a freshly prepared Pt/C catalyst modified GC disk electrode in the presence of various concentrations of AcN. Potential scan rate: 0.1 V s^{-1}.

(commences at ca. 0.75 V and extends up to 1.5 V vs. RHE) coupled with a single reduction peak centered at ca. 0.58 V vs. RHE, in addition to the appearance of the hydrogen adsorption/desorption ($H_{ads/des}$) couple in the potential region between 0.05 and 0.35 V vs. RHE. Similar features are observed for the poisoned Pt/C catalyst (albeit with lower currents) in the presence of AcN (curves b–e) with the appearance of a distinct oxidation peak at ca. 1.4 V vs. RHE which is assigned to the oxidation of adsorbed AcN. Furthermore, a noticeable decrease in the intensity of the Pt-oxide reduction peak is observed with a concurrent lowering in the intensity of the $H_{ads/des}$ peaks. This reflects the adsorption of AcN onto the Pt/C catalyst and thus decreases its accessible electrochemical active surface area (ECSA). A value of ECSA = 64.4 $m^2\ g^{-1}$ Pt is obtained for the unpoisoned Pt/C catalyst based on the H_{des} peak (using a reported value of 210 μC cm^{-2} [28]) which is about one half of that estimated by the CO-stripping (132.6 $m^2\ g^{-1}$ Pt). A similar observation is reported by Mayrhofer et al. [25], in which the difference between the values of ECSA (estimated by both techniques, i.e., H_{ads} and CO stripping) is getting larger for Pt/C catalyst with particle size > 1.4 nm [25]. CVs for the hydrogen adsorption/desorption ($H_{ads/des}$) at the Pt/C catalyst in 0.1 M $HClO_4$ solution containing various amounts of AcN are shown in Fig. 1B. The presence of a minute amount of acrylonitrile as small as 1 ppm caused a paramount decrease in ECSA as depicted from the CV measurements for the $H_{ads/des}$. We have to mention here that the surface coverage (θ) of AcN on Pt/C catalyst has been estimated based on the $H_{ads/des}$ patterns in which the potential was scanned from 0.45 V (at which the faradaic current is close to zero) toward the cathodic direction, i.e., between 0.45 and 0.05 V vs. RHE. The values of θ of AcN are estimated accordingly by monitoring the decrease in the charge of the H_{des} peak (cf. Table 1). Obviously, increasing the AcN concentration causes an increase in θ and a decrease in ECSA. Table 1 lists the values of ECSA and θ for the unpoisoned and poisoned Pt/C catalysts.

3.2. Electrochemical reduction of oxygen

To evaluate the effect of AcN poisoning on the kinetics of the ORR, a steady-state voltammetry was measured in O_2-saturated 0.1 M $HClO_4$ in the presence of various concentrations of AcN. The data are shown in Fig. 2. Note that the GC disk (modified with the Pt/C catalyst) was polarized at 1.05 V vs. RHE for 10 min before each measurement. Curve a shows a typical ORR voltammogram on Pt surface with a single reduction wave starting at ca. 1 V with a fully developed plateau (which starts at ca. 0.7 V and extends up to 0.4 V vs. RHE), concurrently with a minimal Pt ring current (curve a', corresponding to the oxidation of hydrogen peroxide produced at the unpoisoned Pt/C catalyst). This reflects the exclusive 4-electron reduction of O_2 to water at the unpoisoned Pt/C catalyst (cf. Fig. 3). On the other hand, at the poisoned Pt/C catalyst (curves b–e) the following points are remarkable:

(i) The half-wave potential ($E_{1/2}$) and the onset potential of the ORR are negatively shifted to a various extent depending on the concentration of AcN,
(ii) A significant lowering in the limiting current density at the poisoned Pt/C catalyst (curves b–e), with a significant increase in the corresponding ring current (curves b'–e'). These results demonstrate a significant retardation of the ORR in the presence of AcN and a contribution of the 2-electron reduction pathway (i.e., formation of H_2O_2, cf. Fig. 4).
(iii) Furthermore, the unpoisoned Pt/C catalyst supports a current density of 3.4 mA cm^{-2} at 0.82 V (i.e., in the kinetic-controlled current region) which is lowered to 1.7, 0.8, 0.5 and

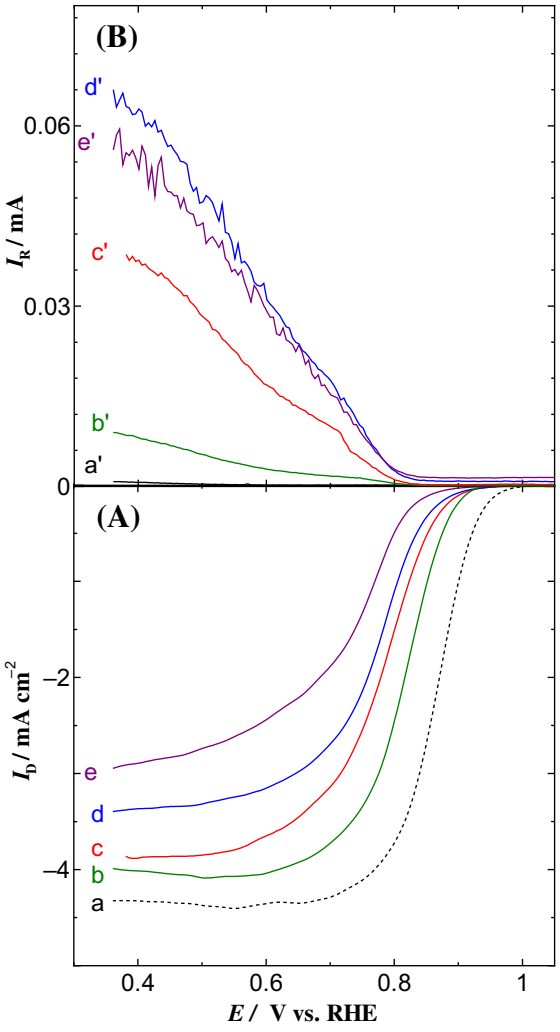

Fig. 2. Steady-state voltammograms (with *IR*-drop corrections) measured at 900 rpm for the ORR at Pt/C catalyst GC disk-Pt ring RRDE electrode in O_2-saturated 0.1 M $HClO_4$ solutions containing (a) 0, (b) 0.5, (c) 1, (d) 10 and (e) 100 ppm AcN. The corresponding Pt ring currents (a'–d') are shown in the upper panel (corresponding to the oxidation of hydrogen peroxide produced at the relevant disk electrode). Potential scan rate: 0.01 V s^{-1}. The Pt ring electrode was potentiostated at 1.25 V vs. RHE. Pt/C loading on the GC disk electrode = 95 μg Pt cm^{-2}.

Table 1
Variation of the electrochemical active surface area (ECSA), surface coverage of acrylonitrile (θ) and shift in the half wave potential ($\Delta E_{1/2}$) of the ORR at Pt/C catalyst in the presence of various concentrations of acrylonitrile. Pt/C loading = 95 μg Pt cm^{-2}.

Solution (0.1 M $HClO_4$ + x ppm acrylonitrile)	ECSA[a] ($m^2\ g^{-1}$ Pt)	θ[b]	$\Delta E_{1/2}$[c] (mV)
0	64.4	0	0
0.5	42.3	34.3	53
1	23.1	64.1	85
10	11.2	82.6	100
100	4.8	92.6	135

[a] As estimated from the amount of charge consumed during the anodic hydrogen desorption (see Fig. 1B) using a reported value of 210 μC cm^{-2} [28].
[b] Estimated from the relation (θ = 1 − ($ECSA_{poisoned}/ECSA_{unpoisoned}$)), where $ECSA_{poisoned}$ and $ECSA_{unpoisoned}$ refer to the electrochemical active surface area of the poisoned and the unpoisoned Pt/C catalyst, respectively.
[c] $\Delta E_{1/2}$ (= $E_{1/2unpoisoned} - E_{1/2poisoned}$) is the negative shift in the half wave potential of the ORR at the poisoned Pt/C catalyst ($E_{1/2poisoned}$) from that observed at the unpoisoned Pt/C catalyst ($E_{1/2unpoisoned}$ = 0.87 V vs. RHE). The values are obtained from Fig. 2.

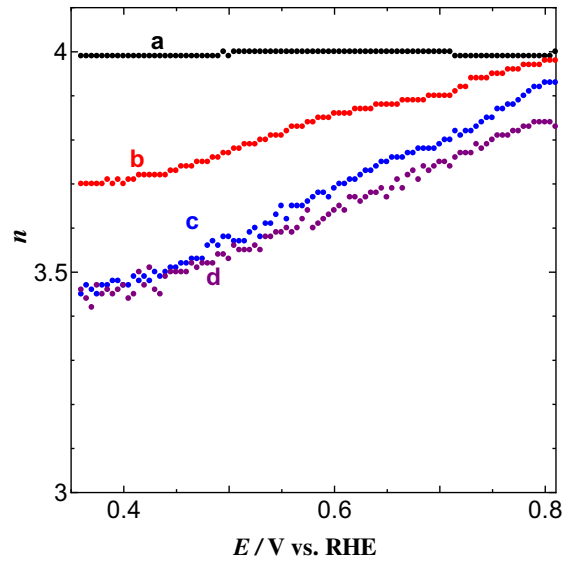

Fig. 3. Variation of the number of the exchanged electrons (n) with the disk electrode potential during the ORR at Pt/C catalysts in in O_2-saturated 0.1 M $HClO_4$ solution containing (a) 0, (b) 1, (c) 10 and (d) 100 ppm AcN. Data were estimated from the corresponding RRDE voltammograms in Fig. 2.

0.2 mA cm^{-2} in the presence of 0.5, 1, 10 and 100 ppm AcN, respectively. This amounts to about 50% loss in the catalytic activity in the presence of 0.5 ppm AcN.

The diffusion-limiting current (i_d) of the ORR is given by [29]:

$$i_d = 0.62nFAD^{2/3}\omega^{1/2}\nu^{-1/6}c^* \quad (1)$$

where c^* is the concentration of dissolved O_2 in 0.1 M $HClO_4$ solution, A is the geometric surface area of the desk electrode, ω is the electrode rotation rate, n is the number of exchanged electrons during the ORR, ν is the kinematic viscosity and other symbols have their usual meanings. The observed decrease of i_d at the poisoned Pt/C catalysts points to a crucial retarding role of AcN in the reduction pathway of O_2 by reducing the number of electrons (n) exchanged during the course of the ORR.

Further analysis of the steady-state voltammograms (shown in Fig. 2) has been carried out by estimation of the values of n and % H_2O_2 produced at the disk electrode during the ORR in 0.1 M $HClO_4$ solution in the presence of various amounts of AcN (Figs. 3 and 4, respectively). Note that n and $\%H_2O_2$ were estimated using Equations (2) and (3), respectively [30]:

$$n = \frac{4I_D}{I_D + \frac{I_R}{N}} \quad (2)$$

and

$$\%H_2O_2 = \frac{\frac{200I_R}{N}}{I_D + \frac{I_R}{N}} \quad (3)$$

where I_R and I_D are the ring and disk currents, respectively, and N is the collection efficiency of the RRDE (= 0.37). Inspection of Fig. 4 reveals a significant contribution of the 2-electron reduction pathway (i.e., hydrogen peroxide) during the course of the ORR in the presence of AcN. That is, at the disk potential of 0.75 V, % $H_2O_2 \cong 0.15\%$ at the unpoisoned Pt/C catalyst and increases up to 3, 7 and 10% in the presence of 1, 10 and 100 ppm AcN, respectively. A monotonic increase of $\%H_2O_2$ is observed over the whole potential range. This finding is consistent with previous reports in which detectable amounts of H_2O_2 are produced at Pt, Pt nanoparticles modified GC and Pt/C cathodes poisoned with various contaminants, e.g., ammonium ions, SO_2 or NOx [8,15,31]. These indicate the predominant retarding effect of the poison against the complete 4-electron reduction of O_2 to water over the whole potential range of the ORR. A so-called dual adsorption of O_2 molecules is likely favorable for the 4-electron reduction of O_2 to H_2O, whereas a single adsorption is probably sufficient for the formation of hydrogen peroxide [32]. Thus, at the poisoned Pt/C catalyst a significant contribution of the end-on (Pauling-model) adsorption mode of O_2 prevails leading to the formation of hydrogen peroxide [12,14,33,34], as a result of the adsorption of AcN on the Pt/C catalyst surface, thus impeding the parallel adsorption mode of O_2 molecules (necessary for O–O bond breaking) [32]. Alternatively, one might consider a contribution of an outer-sphere electron transfer mechanism during the ORR at the poisoned Pt/C catalyst similar to that suggested by Ramaswamy and Mukerjee [35] in which OH species adsorbed at the Pt surface inhibit the direct molecular adsorption of O_2 and promotes a 2-electron reduction of O_2 to hydrogen peroxide. Similarly, the outer-sphere mechanism has been proposed as a plausible reduction pathway of O_2 to superoxide ions (via a one-electron transfer) at thiophenol modified Au electrodes [36] as well as at Hg electrodes modified with hydrophobic film of quinoline derivatives [37].

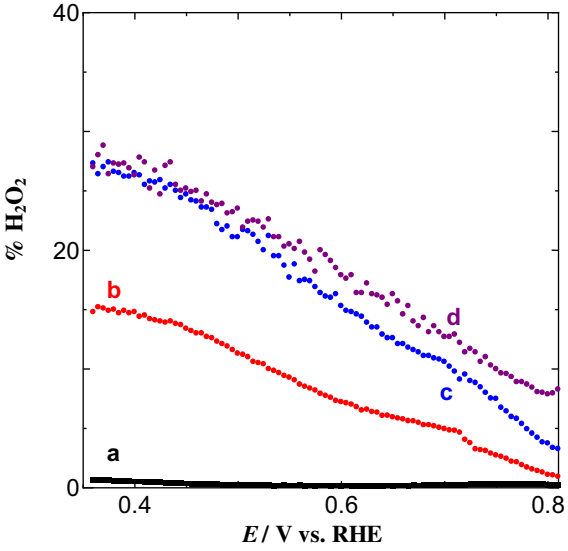

Fig. 4. Variation of the percentage of hydrogen peroxide ($\%H_2O_2$) with the disk electrode potential during the ORR at Pt/C catalysts in O_2-saturated 0.1 M $HClO_4$ solution containing (a) 0, (b) 1, (c) 10 and (d) 100 ppm AcN. Data were estimated from the corresponding RRDE voltammograms in Fig. 2.

3.3. Tafel plots

To further clarify the poisoning effect of AcN, mass-transfer corrected Tafel plots of the ORR at (a) unpoisoned and (b) poisoned Pt/C catalysts are shown in Fig. 5. This figure depicts two different linear regions for each curve with two distinct slopes at low and high current density regions, respectively, i.e., −68 and −128 mV dec^{-1} for the unpoisoned Pt/C catalyst, and −70 and −228 mV dec^{-1} for the poisoned Pt/C catalyst. For the unpoisoned Pt/C, the Tafel slope, in the large overpotential region, is

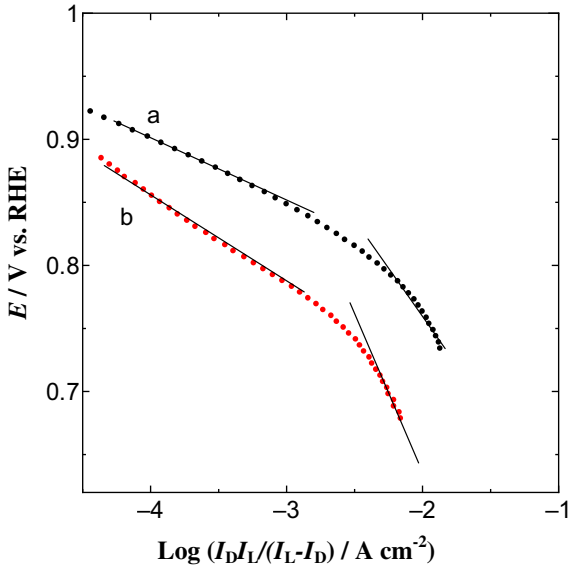

Fig. 5. Mass transfer-corrected Tafel plots for the ORR obtained at Pt/C catalyst in O_2-saturated 0.1 M $HClO_4$ solutions containing (a) 0 and (b) 100 ppm AcN. Note that Tafel plots are corrected for the *IR*-drop using a value of the solution resistance of 14.8 Ω (as estimated from the impedance measurements).

almost double that in the small overpotential region, similar to previous reports [38]. The change in the Tafel slope is related to the change in the nature of the adsorbed oxygen species and the potential-dependent variation of their surface coverage on the electrode surface. [39–41]. The similar Tafel slopes obtained at the poisoned and unpoisoned Pt/C catalysts in the low overpotential region indicates a negligible influence of AcN on the rate-determining step of the ORR, possibly due to the small surface coverage and also its feasible oxidation within this potential range (see Fig. 1A). However, in the large overpotential region, the poisoned Pt/C catalyst shows a larger Tafel slope (−228 mV dec^{-1}) than that obtained at the unpoisoned Pt/C catalyst (ca. −128 mV dec^{-1}), implying that the kinetics of the ORR becomes sluggish in the presence of AcN. The large value of Tafel slope ($b = RT/\alpha nF$) obtained at the poisoned Pt/C catalyst reflects a significant decrease in the value of αn. That is, the transfer coefficient and/or the number of exchanged electrons is being less than those obtained at the unpoisned Pt/C catalyst [42].

This fact points to a crucial role of the surface coverage of AcN at the Pt/C surface in determining its catalytic activity. The variation of θ of AcN with the disk electrode potential could be probed by comparing the values of θ obtained at two different potential regions, namely, at the Pt-oxide reduction region (at ca. 0.6 V, Fig. 1) and at the $H_{ads/des}$ region (in the potential range from ca. 0.02–0.3 V vs. RHE, see Fig. 1). For instance, a value of $\theta = 64\%$ is obtained based on the decrease in the $H_{ads/des}$ peak (in the presence of 1 ppm AcN) compared to a value of $\theta = 41\%$ as estimated from the decrease in the Pt-oxide reduction peak. This finding reflects the potential dependency of θ. That is, the adsorbed AcN molecules could be oxidized and thus a low value of θ is obtained within the potential window of the Pt-oxide formation which is not the case within the $H_{ads/des}$ potential domain (i.e., between 0.45 and 0.05 V vs. RHE). This urged us to compare the RRDE voltammograms of the ORR obtained in the positive-going and negative-going potential scans in O_2-saturated 0.1 M $HClO_4$ solution containing 100 ppm AcN. The results are shown in Fig. 6. Note that, prior to each measurement; the Pt/C catalyst modified GC disk electrode was polarized at (a) 1.05 V and (b) 0.38 V vs. RHE for 10 min. The ring currents (curves a' and b') corresponding to the oxidation of hydrogen peroxide – produced at the relevant disk electrode– are shown in the upper panel. Inspection of this figure reveals that the disk current largely depends on the initial potential of the Pt/C desk a direction of the potential scan. That is a pronounced retarding effect of AcN on the ORR is observed during the positive-going potential excursion (curve b, with an initial holding potential of 0.38 V vs. RHE) compared with that obtained during the negative-going potential scan (curve a, with an initial holding potential of 1.05 V vs. RHE). In the latter case (curve a), the amount of adsorbed AcN decreases upon holding the Pt/C desk at such a high anodic potential (1.05 V vs. RHE) due to its oxidation, while at 0.38 V no significant oxidation of AcN occurs, thus a larger value of θ is obtained and consequently the ORR is more retarded (curve b).

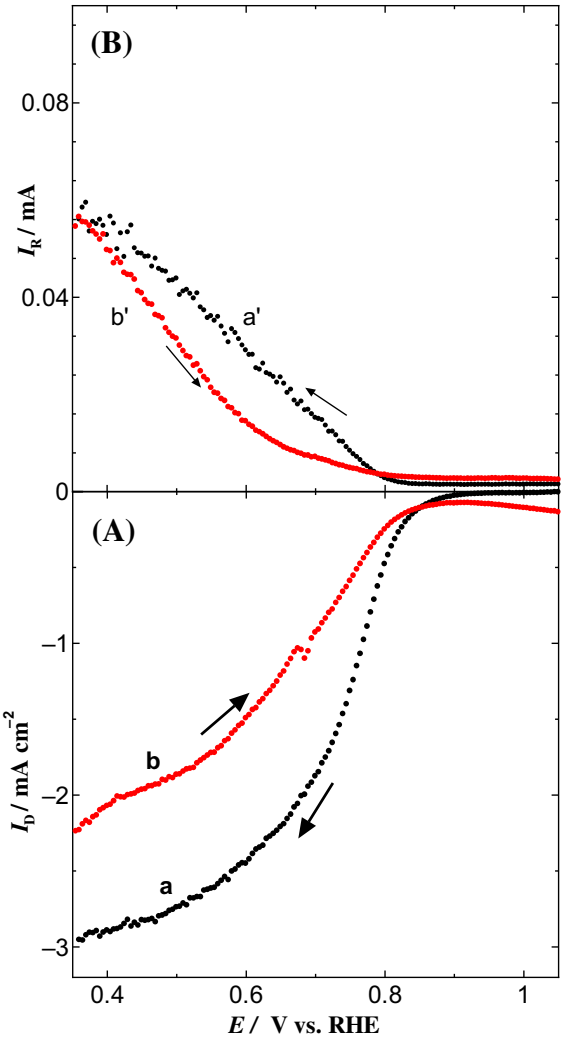

Fig. 6. Comparison of the RRDE voltammograms for the ORR at Pt/C catalyst (loaded on GC disk electrode at 95 μg Pt cm^{-2}) in O_2-saturated 0.1 M $HClO_4$ solution containing 100 ppm AcN at (a) negative-going and (b) positive-going potential scans. The corresponding Pt ring currents (a'–b') are shown in the upper panel (corresponding to the oxidation of hydrogen peroxide produced at the relevant disk electrode). Potential scan rate: 0.01 V s^{-1}. The ring was potentiostated at 1.25 V vs. RHE.

Fig. 7 A and B show the variation of n and $\%H_2O_2$, respectively, with the disk electrode potential during the ORR at a Pt/C catalyst in O_2-saturated 0.1 M $HClO_4$ solution containing 100 ppm AcN during (a) negative-going and (b) positive-going potential excursions. The arrows indicate the direction of the potential scan. At a glance, the amount of H_2O_2 produced, e.g., at a potential of 0.45 V vs. RHE is

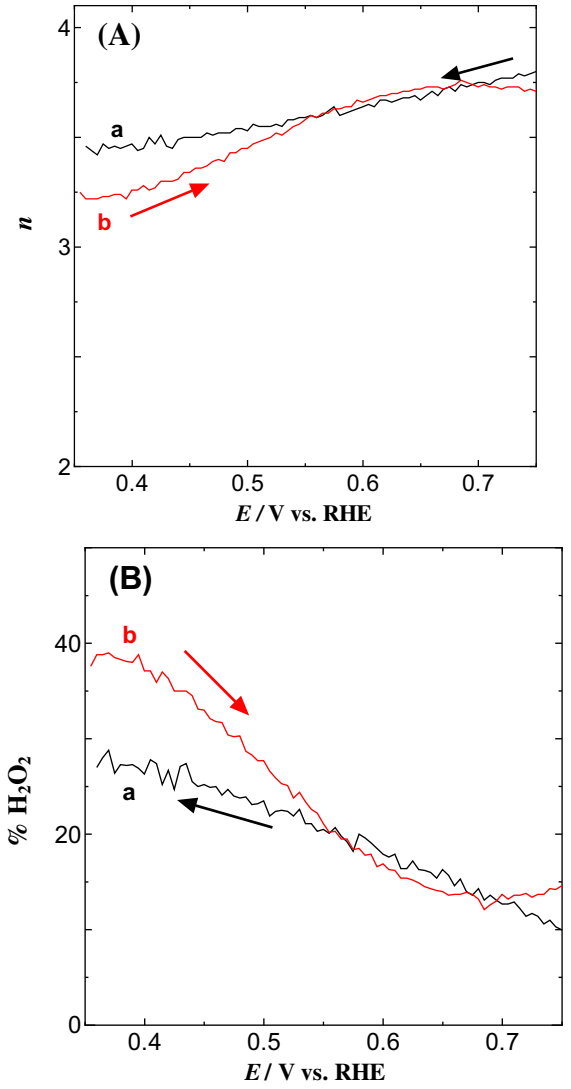

Fig. 7. Variation of (A) n and (B) $\%H_2O_2$ with the disk electrode potential during the ORR at Pt/C catalysts (loaded on GC disk electrode at 95 μg Pt cm^{-2}) in O_2-saturated 0.1 M $HClO_4$ solution containing 100 ppm AcN at (a) negative-going and (b) positive-going potential scans.

larger in the positive-going potential scan (33%) (curve b, panel B) than in the negative-going potential scan (25%) (curve a, panel B). This indicates that a significantly different amount of AcN is adsorbed at the Pt/C catalyst depending on the initial potential of the disk electrode. In other words, the catalytic activity of the Pt/C catalyst is quite sensitive to the direction of potential scan. A similar result was also obtained by considering the variation of n with the direction of potential scan (Fig. 7A).

Fig. 8 shows the relationship between θ (estimated from the $H_{ads/des}$ peaks, Fig. 1B) and $\%H_2O_2$ (obtained from Fig. 4 at 0.45 V vs. RHE) as a function of the concentration of AcN. This figure depicts that both θ and $\%H_2O_2$ increases with the concentration of AcN. Also, it shows a Langmuir-type isotherm in which θ levels off above 100 ppm AcN.

It has been shown that the polarizing potential of a certain electrode is related to changes in the catalyst work function (Φ) [43–45]. Φ is strongly affected by the conditions of the surface of the catalyst. The presence of minute amounts of contaminant (less than a monolayer) can change the work function substantially and in turn the catalytic activity of the catalyst may change. This is a result of the formation of electric dipoles at the surface, resulting

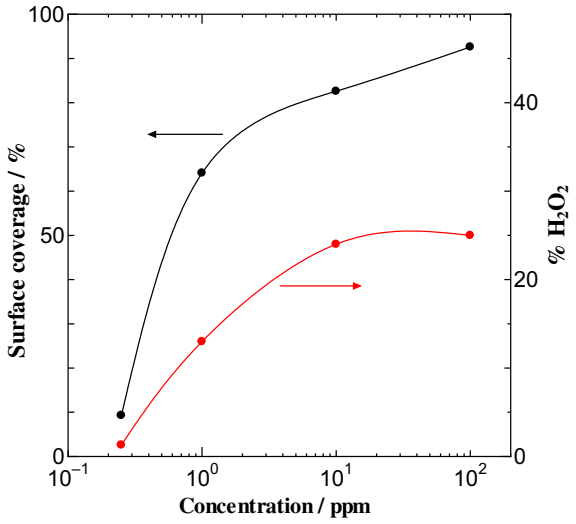

Fig. 8. Surface coverage (θ) of AcN on Pt/C (curve a) and $\%H_2O_2$ (curve b) as a function of the concentration of AcN in O_2-sat. 0.1 M $HClO_4$. Note that the values of θ are estimated from the $H_{ads/des}$ peaks (see Fig. 1B).

in the change in the energy needed for an electron to leave the surface of the catalyst. For instance, methanol adsorption was found to cause a monotonic decrease in Pt work function down to −1.8 eV relative to the clean surface [32]. Thus, the observed retarding in the activity of the poisoned Pt/C catalyst toward the ORR could result from a decrease in the Pt work function due to AcN adsorption. Φ is sensitive to any physicochemical changes on the electrode surface and the change in Φ could be explained based on Equation (4) [43–48]:

$$\Phi = \Phi_0 - 4\pi s\mu \quad (4)$$

where Φ_0 is the work function of the bare metal surface and s is the surface concentration of the adsorbate and μ is the dipole moment of the adsorbate directed perpendicularly to the metal surface. Note that Equation (4) encounters a simplification as it is originally proposed for adsorption at a metal surface (uncharged) in UHV. However, it can be used to predict a qualitative assessment of the retarding effect of the poison. That is, the change in work function of Pt ($\Delta\Phi = \Phi - \Phi_0$) depends on s and μ of the impurity. The increase of the concentration of AcN from 0.5 to 100 ppm increases θ (which is proportional to s), and thus shifts $E_{1/2}$ of the ORR toward the negative direction of potential (see Table 1) along with a noticeable increase in $\%H_2O_2$ (see Fig. 8) as a result of a decrease in n (see Fig. 3).

3.4. Recovery of catalytic activity of the Pt/C catalyst

In order to retrieve ECSA (and in turn the catalytic activity) of the poisoned Pt/C catalyst, the potential of the poisoned Pt/C catalyst electrode was cycled several times within two different potential domains. Firstly, within the potential region of the $H_{ads/des}$, i.e., between 0.45 and 0.05 V vs. RHE, in N_2-saturated 0.1 M $HClO_4$ solution at a potential scan rate of 0.1 V s^{-1}. The percent recovery of ECSA is plotted against the number of potential cycles (Fig. 9, curve a). This figure shows that cycling the potential within the $H_{ads/des}$ region did not lead to a significant regeneration of ECSA of the Pt/C catalyst. Secondly, a repetitive potential cycling between the onset potentials of the hydrogen and oxygen evolution reactions, i.e., between 0.05 and 1.5 V vs. RHE, caused a remarkable retrieval of ECSA of Pt/C catalyst (Fig. 9, curve b). That is, an almost complete recovery of ECSA (>98%) is achieved after 3 potential

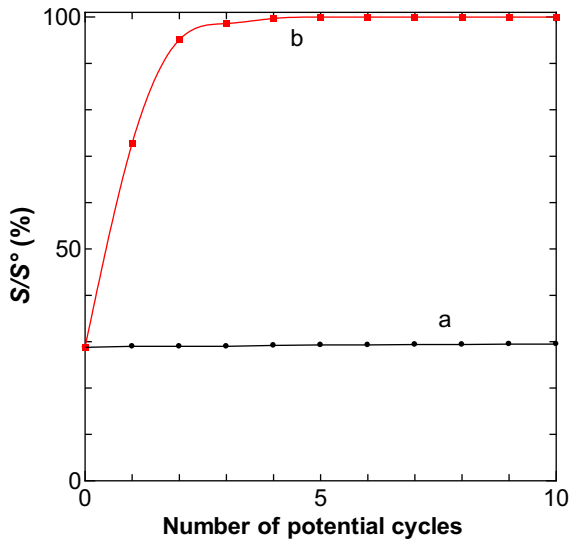

Fig. 9. Variation of the percent recovery (S/S_o) of ECSA of the poisoned Pt/C catalyst with the number of potential cycles between (a) 0.05 and 0.45 V and (b) 0.05 and 1.5 V vs. RHE at 0.1 V s^{-1} in N_2-saturated 0.1 M $HClO_4$ solution. Note that the Pt/C catalyst modified GC disk electrode was pre-poisoned by immersing in 0.1 M $HClO_4$ solution containing 100 ppm AcN at ocp (ca. 0.98 V vs. RHE) for 10 min. Note that S_o and S refer to ECSA of the unpoisoned and the poisoned Pt/C catalysts.

cycles. This indicates that the oxidative removal of AcN is remarkably effective to recover ECSA of the poisoned Pt/C catalyst compared with the removal via a competition with the hydrogen adsorption-desorption.

4. Conclusions

AcN causes a significant retardation of the catalytic activity of the Pt/C catalyst toward the ORR in $HClO_4$ solution to an extent depending on its level of contamination. The adsorption of AcN lowers ECSA of the Pt/C catalyst and is proposed to impede the parallel adsorption mode of oxygen molecules at the Pt/C catalyst (necessary for O–O bond breaking). Accordingly, a significant amount of the 2-electron reduction product, i.e., hydrogen peroxide, is detected. At high current density region, the poisoned Pt/C catalyst exhibits a higher Tafel slope (−228 mV dec^{-1}) than that obtained at the unpoisoned Pt/C catalyst (ca. −128 mV dec^{-1}), implying that the kinetics of the ORR becomes sluggish in such a potential range in the presence of AcN. The increase of the surface coverage of AcN on the Pt surface is thought to alter its work function (Φ) in such a way that the catalytic activity of the Pt/C catalyst toward the ORR deteriorates. Retrieval of ECSA is achieved by employing a few potential cycles between the onset potentials of the hydrogen evolution and oxygen evolution reactions.

Acknowledgments

This work was financially supported by a Grant-in-Aid for Scientific Research (A) (No. 19206079) from the Ministry of Education, Culture, Sports, Science and Technology (MEXT), Japan and also by the New Energy and Industrial Technology Development Organization (NEDO), Japan.

References

[1] Y. Nagahara, S. Sugawara, K. Shinohara, J. Power Sources 182 (2008) 422.
[2] B.D. Gould, O.A. Baturina, K.E. Swider-Lyons, J. Power Sources 188 (2009) 89.
[3] R. Birup, J. Meyers, B. Pivovar, Y. Kim, R. Mukundan, N. Garland, D. Myers, M. Wilson, F. Garzon, D. Wood, P. Zelenay, K. More, K. Stroh, T. Zawodzinski, J. Boncella, J. McGrath, M. Inaba, K. Miyatake, M. Hori, K. Ota, Z. Ogumi, S. Myiata, A. Nishikata, Z. Siroma, Y. Uchimoto, K. Yasuda, K. Kimijima, N. Iwashita, Chem. Rev. 107 (2007) 3904.
[4] J. St-Pierre, M.S. Angelo, Y. Zhai, ECS Trans. 41 (2011) 279.
[5] K. Kobayashi, Y. Oono, M. Hori, ECS Meet. Abstr. (2012) 1291. MA2012-02.
[6] N. Zamel, X. Li, Prog. Energ. Comb. Sci. 37 (2011) 292.
[7] Product information: DupontTM, Nafion®. http://www.fuelcelmarkets.com/content/images/articles//nae101.pdf.
[8] M. Chen, C. Du, J. Zhang, P. Wang, T. Zhu, J. Power Sources 196 (2011) 620.
[9] F. Xie, Z.-G. Shao, G. Zhang, J. Zhai, W. Lu, X. Qin, W. Lin, B. Yi, Electrochim. Acta 67 (2012) 50.
[10] D.E. Ramaker, D. Gatewood, A. Korovina, Y. Garsany, K.E. Swider-Lyons, J. Phys. Chem. C 114 (2010) 11886.
[11] Y. Garsany, O.A. Baturina, K.E. Swider-Lyons, J. Electrochem. Soc. 154 (2007) B670.
[12] A.M. Abdullah, M.M. Saleh, M.I. Awad, T. Okajima, F. Kitamura, T. Ohsaka, J. Solid State Electrochem. 14 (2010) 1727.
[13] M.I. Awad, M.M. Saleh, T. Ohsaka, J. Power Sources 196 (2011) 3722.
[14] J. Fu, M. Hou, C. Du, Z. Shao, B. Yi, J. Power Sources 187 (2009) 32.
[15] R. Halseid, M. Heinen, Z. Jusys, R.J. Behm, J. Power Sources 176 (2008) 435.
[16] R. Mohtadi, W.-k. Lee, S. Cowan, J.W. Van Zee, M. Murthy, Electrochem. Solid-state Lett. 6 (2003) A272.
[17] D.-T. Chin, P.D. Howard, J. Electrochem. Soc. 133 (1986) 2447.
[18] X. Cheng, Z. Shi, N. Glass, L. Zhang, J. Zhang, D. Song, Z.-S. Liu, H. Wang, J. Shen, J. Power Sources 165 (2007) 739.
[19] O.A. Baturina, B.D. Gould, Y. Garsany, K.E. Swider-Lyonsa, Electrochim. Acta 55 (2010) 6676.
[20] J.M. Moore, P.L. Adcock, J.B. Lakeman, G.O. Mepsted, J. Power Sources 85 (2000) 254.
[21] R. Mohtadi, W.-k. Lee, J.W. Van Zee, J. Power Sources 138 (2004) 216.
[22] F. Jing, M. Hou, W. Shi, J. Fu, H. Yu, P. Ming, B. Yi, J. Power Sources 166 (2007) 172.
[23] S. Knights, N. Jia, C. Chuy, J. Zhang, Fuel Cell Seminar: Fuel Cell Progress, Challenges and Markets, Palm Prings, California, 2005.
[24] D. Yang, J. Ma, L. Xu, M. Wu, H. Wang, Electrochim. Acta 51 (2006) 4039.
[25] K.J.J. Mayrhofer, D. Strmcnik, B.B. Blizanac, V. Stamenkovic, M. Arenz, N.M. Markovic, Electrochim. Acta 53 (2008) 3181.
[26] H.A. Gasteiger, S.S. Kocha, B. Sompalli, F.T. Wagner, Appl. Catal. B: Environ. 56 (2005) 9.
[27] K. Ke, K. Hiroshima, Y. Kamitaka, T. Hatanaka, Y. Morimoto, Electrochim. Acta 72 (2012) 120.
[28] S. Trasatti, O.A. Petrii, Pure Appl. Chem. 93 (1991) 711.
[29] N.M. Marković, H.A. Gasteiger, B.N. Grgur, P.N. Ross, J. Electroanal. Chem. 467 (1999) 157.
[30] M.S. El-Deab, T. Sotomura, T. Ohsaka, Electrochem. Commun. 7 (2005) 29.
[31] M.R. Rahman, M.I. Awad, F. Kitamura, T. Okajima, T. Ohsaka, J. Power Sources 220 (2012) 65.
[32] R. Adzic, in: J. Lipkowski, P.N. Ross (Eds.), Electrocatalysis, Wiley-VCH, New York, 1998 (Chap. 5).
[33] T.J. Schmidt, U.A. Paulus, H.A. Gasteiger, R.J. Behm, J. Electroanal. Chem. 508 (2001) 41.
[34] N.M. Marković, P.N. Ross, Surf. Sci. Rep. 45 (2002) 117.
[35] N. Ramaswamy, S. Mukerjee, J. Phys. Chem. C 115 (2011) 18015.
[36] F. Matsumoto, K. Tokuda, T. Ohsaka, Electrochemistry 63 (1995) 1205.
[37] F. Matsumoto, K. Tokuda, T. Ohsaka, Electroanalysis 8 (1996) 648.
[38] J.X. Wang, F.A. Uribe, T.E. Springer, J. Zhang, R. Adzic, Faraday Discuss. 140 (2009) 347.
[39] R. Halseid, T. Bystron, R. Tunold, Electrochim. Acta 51 (2006) 2737.
[40] L.M. Vracar, N.V. Krstajic, V.R. Radmilvoic, M.M. Jasic, J. Electroanal. Chem. 587 (2006) 99.
[41] F.H. Lima, M.L. Calegaro, E.A. Ticianelli, Russ. J. Electrochem. 42 (2006) 1283.
[42] W.E. Mustain, J. Prakash, J. Power Sources 170 (2007) 28.
[43] C.G. Vayenas, S. Bebelis, I.V. Yentekakis, H.-G. Lintz, Catal. Today 11 (1992) 303.
[44] C.G. Vayenas, S. Bebelis, S. Ladas, Nature 343 (1990) 625.
[45] C.G. Vayenas, S. Bebelis, M. Despotopoulou, J. Catal. 128 (1991) 415.
[46] S. Trasatti, Surf. Sci. 335 (1995) 1 (And the references cited therein).
[47] H. Alqahtany, P.-H. Chiang, D. Eng, M. Stoukides, Catal. Lett. 13 (1992) 289.
[48] W. Schmickler, J. Electroanal. Chem. 249 (1988) 25.